Fibrillisation of Hydrophobically Modified Amyloid Peptide Fragments in an Organic Solvent

M.J.Krysmann, V.Castelletto and I.W.Hamley*

Dept of Chemistry, The University of Reading, Reading RG6 6AD, UK

* Author for correspondence. Electronic address: I.W.Hamley@reading.ac.uk

1

Abstract

The self-assembly of a hydrophobically modified fragment of the amyloid β peptide has been studied in methanol. The peptide FFKLVFF is based on Aβ(16-20) extended at the N terminus by two phenylalanine residues. The formation of amyloid-type fibrils is confirmed by congo red staining, thioflavin T fluorescence and circular dichroism experiments. FTIR points to the formation of β-sheet structures in solution and in dried films and suggests that aggregation occurs at low concentration and is not strongly affected by further increase in concentration, i.e. the peptide is a strong fibril-former in methanol. UV fluorescence experiments on unstained peptide and CD point to the importance of aromatic interactions between phenylalanine groups in the aggregation into β-sheets. The CD spectrum differs from that usually observed for β-sheet assemblies formed by larger peptides or proteins and this is discussed for solutions in methanol and also trifluoroethanol. The fibril structure is imaged by transmission electron microscopy and scanning electron microscopy on dried samples and is confirmed by small-angle x-ray scattering experiments in solution.

1. Introduction

The self-assembly of biological materials is fast becoming a major field of broad interest to researchers in soft matter science.[1] This is motivated by the immense interest in the development of peptide-based biomaterials such as hydrogels, drug delivery agents, templates for inorganic materials synthesis, organogelators etc. The present paper concerns the self-assembly of a novel hydrophobically modified peptide in an organic solvent. It forms part of a program of research aimed firstly at understanding the factors responsible for amyloid fibril formation, and second the development of strategies to hinder amyloid formation by design of short peptide fragments and copolymers that bind to the native peptide and disrupt fibrillisation.

The formation of fibrils is symptomatic of many amyloid diseases such as Alzheimer's and Creutzfeldt-Jacob disease.[2] Due to its relevance to a diverse number of conditions affecting large numbers of people, fibril formation by the amyloid beta peptide has been widely studied. There are two variants of the amyloid peptide in humans – Aβ(1-40) and Aβ(1-42) of which the latter is believed to be more susceptible to fibrillisation.[3]

The fibrillisation of several fragments of Aβ(1-40) and Aβ(1-42) has been investigated by a number of groups. Early work has been reviewed elsewhere.[4, 5] The results of experimental and modelling work by several groups[6-18] suggests that sequence Aβ(16-20) i.e. KLVFF is critical for fibrillisation. This work has recently been reviewed.[19]

In this paper, we present results on the fibrillisation of a modified fragment of Aβ(1-42), specifically sequence Aβ(16-20) extended by two hydrophobic residues on the N-terminal side to give FFKLVFF. This was motivated by our efforts to develop a hydrophobic peptide fragment that may act as an organogelator. In addition, we are exploring the role of aromatic interactions on peptide self-assembly through the design of model peptides (future work will include discussion of analogues in which the F residues are replaced by A). Fibrillisation in methanol is confirmed by congo red staining, thioflavin T fluorescence and electron microscopy (SEM and TEM). Small-angle x-ray and neutron scattering provide additional information on fibril dimensions. The secondary structure of the peptide aggregates is studied by circular dichroism and FTIR spectroscopy. Since FFKLVFF does not dissolve in water and is designed to self-assemble in organic solvents, comparison with KLVFF does not seem meaningful. In addition, as mentioned above, the aqueous self-assembly of KLVFF itself has already been investigated extensively.

2. Experimental Section

Materials. FFKLVFF (Scheme 1) was synthesized by solid phase methods using standard FastMoc (Fmoc - 9-fluorenylmethyloxycarbonyl protecting group and activation by HBTU) chemistry. Amino acids (Fmoc-Lysine(Boc)-OH, Fmoc-Leucine-OH, Fmoc-Valine-OH, Fmoc-Phenylalanine-OH), Fmoc-Phenylalanine-Wang resin and HBTU (2-(1H-benzotriazol-1-yl)-1,1,3,3-tetramethyluronium hexafluorophosphate) were purchased from Novabiochem (United Kingdom). HOBt/DMF (mixture of 1-hydroxybenzotriazole and dimethylformamide), DIEA/NMP (mixture of diisopropylethylamine and N-methylpyrrolidone) and NMP

were obtained from Applied Biosystems (United Kingdom). Water (HPLC grade), acetonitrile (HPLC grade), acetic acid and diethyl ether were purchased from Fluka (United Kingdom). Piperidine, trifluoroacetic acid (TFA), triisopropylsilane, α-cyano-4-hydroxy-cinnamic acid, sodium trifluoroacetate, methanol, trifluorethanol and all other reagents were purchased from Sigma-Aldrich (United Kingdom) and were of the highest purity.

The peptide was synthesized on a 0.25 mmol scale using a fully automated peptide synthesizer (433A Applied Biosystems, United Kingdom) which allowed for direct conductivity monitoring of Fmoc deprotection.

The resin to be used for FFKLVFF peptide synthesis was Fmoc-Phenylalanine-Wang resin with 0.74 mmol/g substitution. The peptide was assembled from the C-terminal towards the N-terminal, and was attached to the solid support at the C-terminal by the α-carbonyl group of the amino acid. According to the standard FastMoc protocol, the first step of the reaction was to remove the Fmoc protecting group from the amino acid by a solution of piperidine in NMP. The next step was activation of the carbonyl group of the new amino acid (dissolved in NMP) using HBTU (dissolved in HOBt, DIEA and DMF). The activated amino acid was transferred from the activation vessel to the reaction vessel containing the previously deprotected amino terminal group of the peptide chain and coupling was performed. To obtain the highest coupling efficiency, four times excess of each amino acid was used in 0.25 mmol cycles. Peptide attached to the solid support was obtained from the synthesizer. In the cleavage step a mixture of 95% TFA, 2.5% triisopropylsilane and 2.5% water was used. The sample was occasionally shaken at room temperature for approximately 4 hours and the insoluble resin was washed with TFA. The peptide solution was precipitated in ice cold diethyl ether. Sample was separated by centrifugation and the

solvent was decanted. The solid peptide was washed with diethyl ether and dried. During the cleavage the side chain protecting groups (Boc) were removed by TFA. The crude peptide was purified by reverse phase high performance liquid chromatography (RP-HPLC; Beckman System Gold with Programmable Solvent Module 126 and Diode Array Detector Module 168) using a C18 preparative column (Supelco), for 30min with flow rates 2.5mL/min. A mobile phase of 75/25 (v/v) water/acetic acid and acetonitrile with 0.1% TFA was used. Sample elution was monitored by using a UV/VIS detector operating at 210 nm and 254 nm. The sample dissolved in HPLC solvents was freeze dried. Molecular weight was determined by MALDI-TOF mass spectrometry (Matrix-assisted laser desorption-ionization time-of-flight; Laser ToF SAI – LT3). As a matrix α-cyano-4-hydroxy-cinnamic acid dissolved in methanol was used. Sodium trifluoroacetate was added to facilitate ionization.

MALDI TOF (m/z): 947.97 (+Na=23) [expected: 947.20] The ^{1}H NMR spectra in DMSO were measured with Bruker AMX 400 instrument. The unambiguous assignments of proton shifts were made by comparing with homonuclear and heteronuclear correlation spectra (COSY, HETCOR, TOCSY) of KLVFF.

^{1}H NMR (400 MHz DMSO, ppm): 0.71[d, 6H, 2xCH$_3$ (Val) J_1=6.7 Hz]; 0.84 [dd, 6H, 2xCH$_3$ (Leu) J_1=6.5 Hz, J_2=17.9 Hz]; 1.22-1.70 [m, 9H, 4xCH$_2$ (Lys, Leu) CH (Leu)]; 1.86 [dd, 1H, CH (Val) J_1=6.82 Hz, J_2=13.61 Hz]; 2.67-3.18 [m, 10H, CH$_2$ (Lys, Phe)]; 3.96 [dd, 1H, CHα (Lys) J_1=4.29 Hz, J_2=8.04 Hz]; 4.12 [dd, 1H, CHα (Val) J_1=6.9 Hz, J_2=9.0 Hz]; 4.27-4.67 [m, 5H, CHα, (Leu, Phe)]; 7.11-7.35[m, 20H, arom. (Phe)]; 7.68, 7.98, 8.07, 8.21, 8.35, 8.70 [6d, 10H, NH, NH$_2$ (Lys, Leu, Val, Phe) J_1= 9.0 Hz, J_2=8.4 Hz, J_3=8.1 Hz, J_4=7.6 Hz, J_5=8.0 Hz, J_6=7.7 Hz].

Circular Dichroism. The circular dichroism (CD) spectra were recorded on a Chirascan spectropolarimeter (Applied Photophysics, UK). Samples were dissolved in methanol (0.006% wt) and trifluorethanol (0.036% wt), filtered through a 0.2 μm syringe filter and loaded into a 0.1 mm quartz cover slip cuvette. Spectra were obtained from 190 to 250 nm with a 0.5 nm step, 1 nm bandwidth and 1 second collection time per step at 20 °C, taking five averages.

Fourier Transform Infrared spectroscopy. IR spectra in the amide band regions were recorded on a FTIR spectrometer equipped with a DTGS detector. FFKLVFF solution in d_4-methanol (0.5% and 1% wt) was sandwiched between two CaF_2 plate windows (spacer 0.006 mm) and a solid film of dry peptide was deposited on one CaF_2 plate by drying the same solution. Spectra were scanned 64 times over the range of 4000-400 cm^{-1}. Spectral Manager for Windows was used for data acquisition and handling.

Electron Microscopy. TEM and ESEM were performed in the Centre for Advanced Microscopy at the University of Reading. A Philips CM20 transmission electron microscope (TEM), operated at 80kV, was used to study and record images of the FFKLVFF. A droplet of the sample (0.08% and 0.16% wt in MeOH) was placed on polyvinyl formal grids (Agar Scientific, UK), stained with methylamine tungstate (1% wt) (Agar Scientific, UK) and dried.

A FEI Quanta FEG 600 Environmental Scanning Electron Microscope (ESEM) was used to study and record SEM images of the FFKLVFF. A couple of droplets of the sample (0.08 and 0.5% wt in MeOH) were placed on a stub covered with a carbon tab (Agar Scientific, UK) and dried. Samples were investigated with and without gold coating. The experiment was performed under low vacuum for uncoated samples and under high vacuum for gold coated samples.

Polarised Optical Microscopy. Dried samples were stained with freshly prepared and filtered Congo Red solution (the solution of 0.5g Congo red powder suspended in 80 mL of absolute EtOH was combined with 2g of sodium chloride dissolved in 20 mL double-distilled deionized water)[20] and placed onto glass microscope slide and dried. Images of sample placed between crossed polarised were obtained with an Olympus CX-41 microscope.

Congo Red spectroscopic assay. The UV-Vis spectrophotometer, with the baseline measured for 3 mL of PBS pH 7.4 in a disposable cuvette, was used. A fresh solution of Congo Red (7mg/mL) was prepared in PBS, filtered through a 0.2 μm syringe filter and added (15μL) to the PBS pH 7.4 solution. The spectrum was recorded between 400 and 700 nm with a 0.5 nm step, 1 nm bandwidth and 1 second collection time per step. The Congo Red in PBS solution was titrated with 15 μL portions of FFKLVFF (0.25% wt) in methanol and incubated for 30min at room temperature. The spectra were recorded and background subtracted using a Congo Red spectrum in PBS.

Thioflavin T spectroscopic assay. The fluorescence spectroscopy was performed on Perkin Elementar Luminescence spectrometer LS50B in a 1.0 cm quartz cuvette. Freshly prepared stock solution (ThT 8mg/10 mL PBS pH 7.4) was filtered through a 0.2 μm syringe filter and diluted into the PBS pH 7.4 (1mL to 50 mL). The fluorescence intensity was measured for 1 mL of working solution by excitation at 440nm (slitwidth 5nm) and emission 482 nm (slitwidth 10 nm).[20] The ThT solution was titrated with 15 μL portions of FFKLVFF (0.25% wt) in methanol. The spectra were recorded from 450 to 550 nm, taking twenty averages at room temperature and background subtracted using the ThT spectrum in PBS.

Fluorescence spectroscopy. The FFKLVFF aromatic interaction fluorescence was also studied in a 1.0 cm quartz cuvette. The fluorescence intensity was measured for

methanol and methanol with 40 and 120 μL of FFKLVFF (0.0025% wt) in methanol by excitation at 265nm (slitwidth 5nm). The spectra were recorded from 280 to 500 nm, taking twenty averages at room temperature and the background was subtracted.

Small-Angle X-ray Scattering (SAXS). SAXS experiments were performed on beamline ID02 at the European Synchrotron Radiation Facility, Grenoble, France. Samples were placed in sealed cells (1mm path length) in an O-ring between mica windows. Temperature control was achieved using a Peltier device. A CCD detector was used to collect two-dimensional images which were reduced by radial integration to one-dimensional profiles. The sample-detector distance was 2m. Subtraction of background scattering using an appropriate pure solvent reference was performed for the data presented here.

3. Results and Discussion

Fibril Formation

Amyloid-type fibril formation by FFKLVFF was confirmed by the classical techniques[19, 20] used to assay amyloid formation, i.e. Congo Red staining (with UV-vis aborption spectroscopy and polarized optical microscopy) and ThT fluorescence. The peptide, being insoluble in water, was dissolved in methanol. For the polarised optical microscopy, a dried film of the methanol solution was used directly.

Figure 1 shows a polarized optical microscopy of a sample stained with Congo Red. Regions exhibiting green birefringence (5-10 μm in length) are diagnostic of amyloid formation. The UV-vis absorption spectrum shown in Figure 2 confirms the binding of Congo Red by the peptide since the peak at 540 nm (Figure 2b) increases in intensity with peptide concentration.

Thioflavin T fluorescence experiments show a broad emission peak centred at 480 nm (Figure 3), the intensity of which increases with peptide concentration in the solution. This is indicative of binding of the ThT to the peptide and is consistent with "amyloid" formation.[20] We also performed fluorescence experiments on the peptide alone and found a peak at 311 nm due to aromatic interactions, as shown in Figure 4.

Secondary Structure

The secondary structure of peptide FFKLVFF was assessed using circular dichroism and Fourier transform infra-red spectroscopies. Since FFKLVFF is insoluble in water, organic solvents were used for subsequent studies. CD spectra obtained in methanol and TFE solutions are shown in Figure 5. The maximal peptide concentration that could be used was set by the absorbance monitored on the CD spectrometer. The final concentration was greater in TFE than in methanol due to the high absorbance of the alcohol. An additional reason to use low concentrations was to reduce light scattering effects. For the TFE solution this was less of a problem because TFE acts as a strong solvent.

The CD spectrum in TFE shows clearly resolved peaks at 200 nm and 218 nm. A very similar spectrum has recently been reported for a diphenylalanine-based dipeptide[21] and may be characteristic of peptides in which self-assembly is driven by stacking of Phe units. The peak at 200 nm is associated with a π-π* transition and that at 218 nm with a n-π* transition.[21] The CD spectrum obtained for FFKLVFF in methanol seems to be dominated by the maximum at 203 nm, although there is an extended shoulder at higher wavelengths. It is interesting that self-assembly is observed at very low concentrations in methanol, 0.006 wt%. This suggests that the fibril critical

aggregation concentration is even lower, and that FFKLVFF is a "strong fibrilliser" in methanol.

The main focus of the FTIR experiments was on the amide I band, which is sensitive to secondary structure. Additional peaks were located in the amide A band at 3275 cm^{-1} and amide B band at 3087 and 3068 cm^{-1}. A sharp absorption at 3032 cm^{-1} was due to stretching vibration from the benzene rings. A peak at 2958 cm^{-1} was due to the CH_3 vibration. The peak at 2932 cm^{-1} was assigned to the CH_2 asymmetric stretching bands while the peak at 2874 cm^{-1} was due to the CH_3 symmetric stretching bands. The peaks at 1685 and 1623 cm^{-1} were assigned with the amide I band and the peaks at 1544 and 1457 cm^{-1} were signed to amide II band. The CN and CO stretching bands correspond respectively to peaks at 1209 and 1144 cm^{-1}. The peaks in the region 699-839 cm^{-1} are due to deformation vibration of aromatic side groups[22, 23]

FTIR spectra in the amide I region are shown in Figure 6 for solutions with two different concentrations and a dried film. The spectra are quite similar in solution and in the dried film. This suggests that self-assembly has already occurred for concentrations as low as 0.5% peptide and that this is not affected by further increase in methanol concentration, what confirm our earlier study. Moreover, as we know that the fibrils were present in that concentration, we were expecting to interrelate the secondary structure with the fibril formation. The peaks at 1685 and 1623 cm^{-1} (Figure 6) are associated with a β-sheet structure.[22, 24] The higher frequency peaks are often associated with an antiparallel β-sheet structure, although they could also be due to turns or bends,[25] although this seems unlikely in such a short peptide. The ratio between the two peaks indicates the parallel β - sheet secondary structure. A broad

maximum at 1674 suggest turns but can also result from residual TFA left from the HPLC solvent.[26]

In summary, CD and FTIR spectroscopies indicate a β-sheet secondary structure in which self-assembly is driven by aromatic interactions between Phe residues.

Self-organisation of FFKLVFF

The structure of FFKLVFF was investigated by TEM and SEM for dried films and by SAXS to probe self-assembly in solution.

As noted above, CD reveals that FFKLVFF forms fibrils at very low concentration. The formation of fibrils was confirmed directly by TEM. Figure 7 shows images obtained for films prepared from a 0.16% wt solution of the peptide in methanol. This shows fibrillar aggregates at very low concentration. Apart from the 10-20 nm wide fibrils (average width 15 nm), tape-like aggregates, and twisted ribbons were also observed. We note that drying effects during TEM sample preparation can affect fibrillisation of peptides, and certainly the initial concentrations are not too meaningful. We use small-angle x-ray scattering as a direct probe of fibril formation in solution (*vide infra*).

Figure 8 shows images from SEM. Figure 8a,b shows images for samples observed in an SEM instrument under low vacuum conditions. A fibrillar network structure is apparent; the fibrils observed are bundles of the fibrils observed by TEM, the average thickness of the bundles in SEM being 70-160nm. Figure 8c shows an image for a sample (0.5% wt) coated with gold (to improve conductivity) and imaged under conventional high vacuum SEM conditions. The fibrillar structure is better resolved.

The fibril dimensions 33-50 nm are similar to those for the samples measured under low vacuum conditions

SAXS experiments were performed to probe the self-assembled structure in solution. Figure 9 presents data for a 1% solution in methanol. The result obtained is consistent with a significant fraction of fibrillar structures coexisting with larger-scale aggregates. The average fibril width of 15 nm obtained from TEM was used as an input to model SAXS data in Figure 9. This fibril radius was used as an input to model the form factor, represented by a polydisperse cylinder form factor[27]:

$$I(q) \sim \frac{\pi}{q} \int_0^\infty \left[J_1^2(qR) / (q^3 R^2) \right] \exp[-(R - R_c)^2 / 2\sigma^2] dR$$

Here $q = 4\pi \sin\theta / \lambda$ is the wavenumber (2θ and λ are scattering angle and wavelength respectively), J_1 is the first order Bessel function, R_c is the cylinder radius and σ is the polydispersity obtained from the width of the Gaussian function.

This model describes the data quite well as evident in Figure 9 (the polydispersity in radius is 21%). To describe the data at low q, it is necessary to allow for Guinier-type scattering from larger aggregates with $R_g = 23.8$ nm. A background scattering of the form $k.q^{-c}$ where k and c are constants was also included in the model.

4. Summary

We have shown that modification of a fragment of the Aβ peptide, via addition of two phenylalanine residues at the N terminus leads to a hydrophobic peptide that fibrillises

in organic solvent. The peptide is a strong fibrilliser in methanol with a low critical aggregation concentration, below 0.08 wt%. The combination of circular dichroism and fluorescence experiments suggest that the β-sheet structure self-assembles due to aromatic interactions between phenylalanine residues. The fibrillar structure was imaged by TEM and SAXS performed on solutions confirmed that drying does not significantly influence the tendency to form fibrils. Our results indicate that rational modification of peptide fragments is possible to produce peptides that self-assemble in specific solvents.

References

[1] I. W. Hamley and V. Castelletto, *Angewandte Chemie, International Edition in English*, 2007, **46**, 4442.

[2] M. Goedert and M. G. Spillantini, *Science*, 2006, **314**, 777.

[3] P. T. Lansbury and H. A. Lashuel, *Nature*, 2006, **443**, 774.

[4] D. B. Teplow, *Amyloid: International Journal of Experimental and Clinical Investigation*, 1998, **5**, 121.

[5] L. C. Serpell, *Biochimica et Biophysica Acta*, 2000, **1502**, 16.

[6] C. Hilbich, B. Kisterswoike, J. Reed, C. L. Masters, and K. Beyreuther, *Journal of Molecular Biology*, 1992, **228**, 460.

[7] S. J. Wood, R. Wetzel, J. D. Martin, and M. R. Hurle, *Biochemistry*, 1995, **34**, 724.

[8] L. O. Tjernberg, J. Naslund, F. Lindqvist, J. Johansson, A. R. Karlstrom, J. Thyberg, L. Terenius, and C. Nordstedt, *Journal of Biological Chemistry*, 1996, **271**, 8545.

[9] L. O. Tjernberg, C. Lilliehook, D. J. E. Callaway, J. Naslund, S. Hahne, J. Thyberg, L. Terenius, and C. Nordstedt, *Journal of Biological Chemistry*, 1997, **272**, 12601.

[10] L. O. Tjernberg, D. J. E. Callaway, A. Tjernberg, S. Hahne, C. Lilliehöök, L. Terenius, J. Thyberg, and C. Nordstedt, *Journal of Biological Chemistry*, 1999, **274**, 12619.

[11] M. A. Findeis, G. M. Musso, C. C. Arico-Muendel, H. W. Benjamin, A. M. Hundal, J. J. Lee, J. Chin, M. Kelley, J. Wakefield, N. J. Hayward, and S. M. Molineaux, *Biochemistry*, 1999, **38**, 6791.

[12]   D. J. Gordon, K. L. Sciarretta, and S. C. Meredith, *Biochemistry*, 2001, **40**, 8237.

[13]   D. J. Gordon, R. Tappe, and S. C. Meredith, *Journal of Peptide Research*, 2002, **60**, 37.

[14]   J. J. Balbach, Y. Ishii, O. N. Antzutkin, R. D. Leapman, N. W. Rizzo, F. Dyda, J. Reed, and R. Tycko, *Biochemistry*, 2000, **39**, 13748.

[15]   A.-M. Fernandez-Escamilla, F. Rousseau, J. Schymkowitz, and L. Serrano, *Nature Biotechnology*, 2004, **22**, 1302.

[16]   F. Rousseau, J. Schmykovitz, and L. Serrano, *Current Opinion in Structural Biology*, 2006, **16**, 118.

[17]   A. P. Pawar, K. F. DuBay, J. Zurdo, F. Chiti, M. Vendruscolo, and C. M. Dobson, *Journal of Molecular Biology*, 2005, **350**, 379.

[18]   Y. Kallberg, M. Gustafsson, B. Persson, J. Thyberg, and J. Johansson, *Journal of Biological Chemistry*, 2001, **276**, 12945.

[19]   I. W. Hamley *Angewandte Chemie, International Edition in English*, 2007, **in press**.

[20]   M. R. Nilsson, *Methods*, 2004, **34**, 151.

[21]   M. Gupta, A. Bagaria, A. Mishra, P. Mathur, A. Basu, S. Ramakumar, and V. S. Chauhan, *Advanced Materials*, 2007, **19**, 858.

[22]   B. Stuart, 'Biological Applications of Infrared Spectroscopy', Wiley, 1997.

[23]   S.-Y. Lin and H.-L. Chu, *International Journal of Biological Macromolecules*, 2003, **32**, 173.

[24]   P. Haris and D. Chapman, *Biopolymers*, 1995, **37**, 251.

[25]   A. Barth and C. Zscherp, *Quarterly Reviews of Biophysics*, 2002, **35**, 369.

[26]   J. H. Collier and P. B. Messersmith, *Advanced Materials*, 2004, **16**, 907.

27   J. S. Pedersen, *Advances in Colloid and Interface Science*, 1997, **70**, 171.
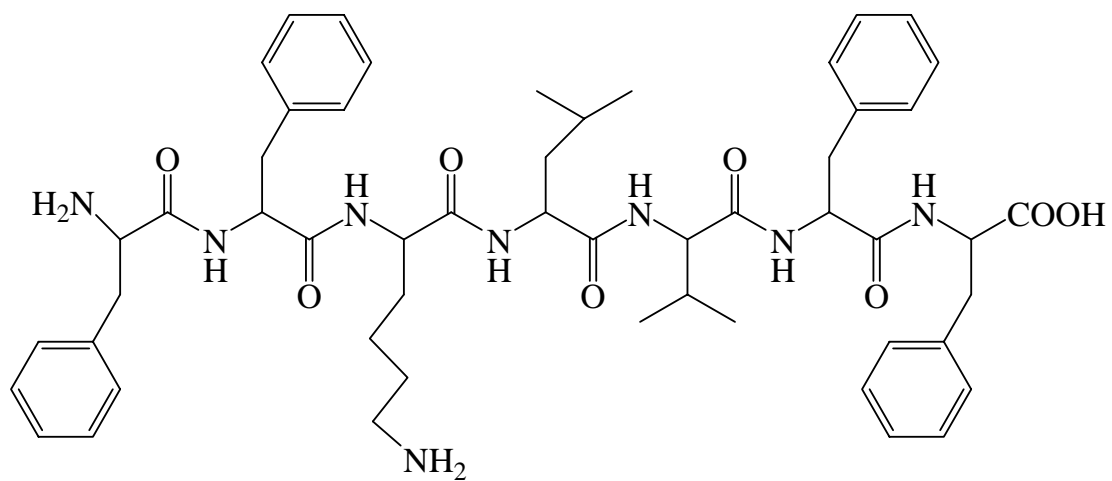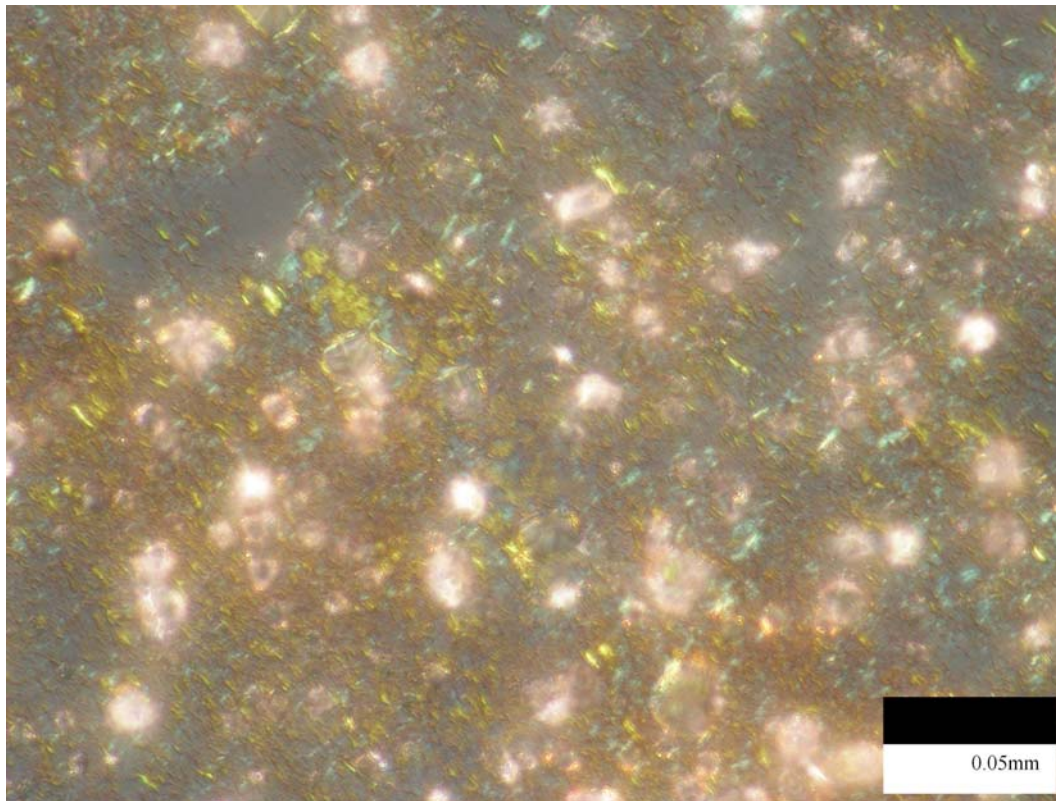
Scheme 1. Molecular structure of FFKLVFF

Figure 1. Polarized optical microscopy image of FFKLVFF stained with Congo Red

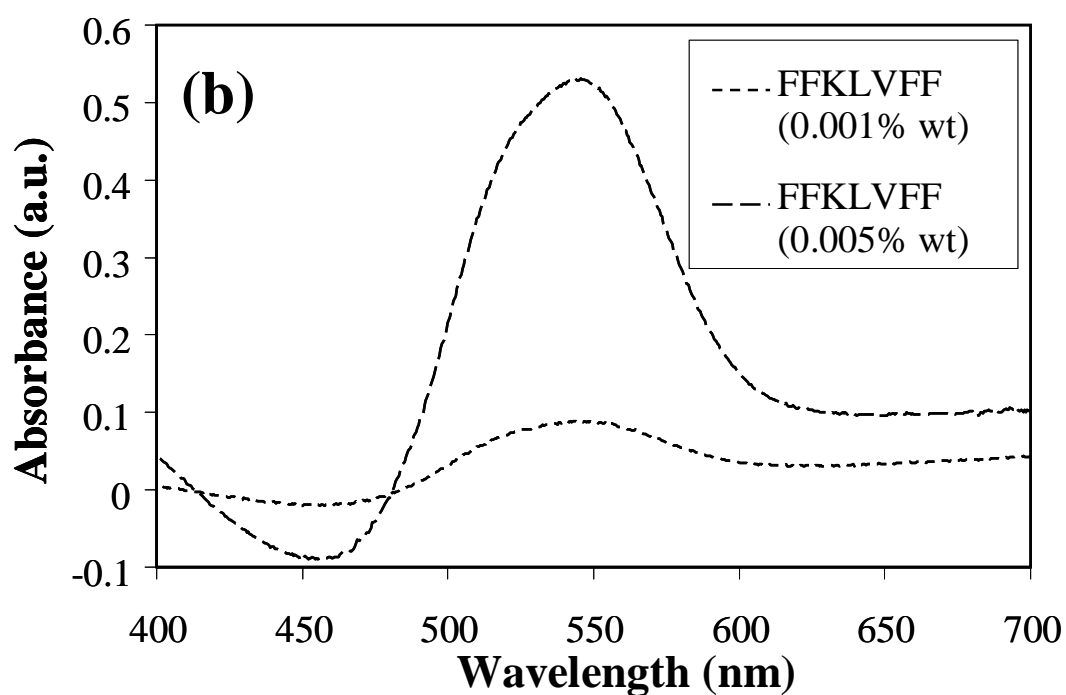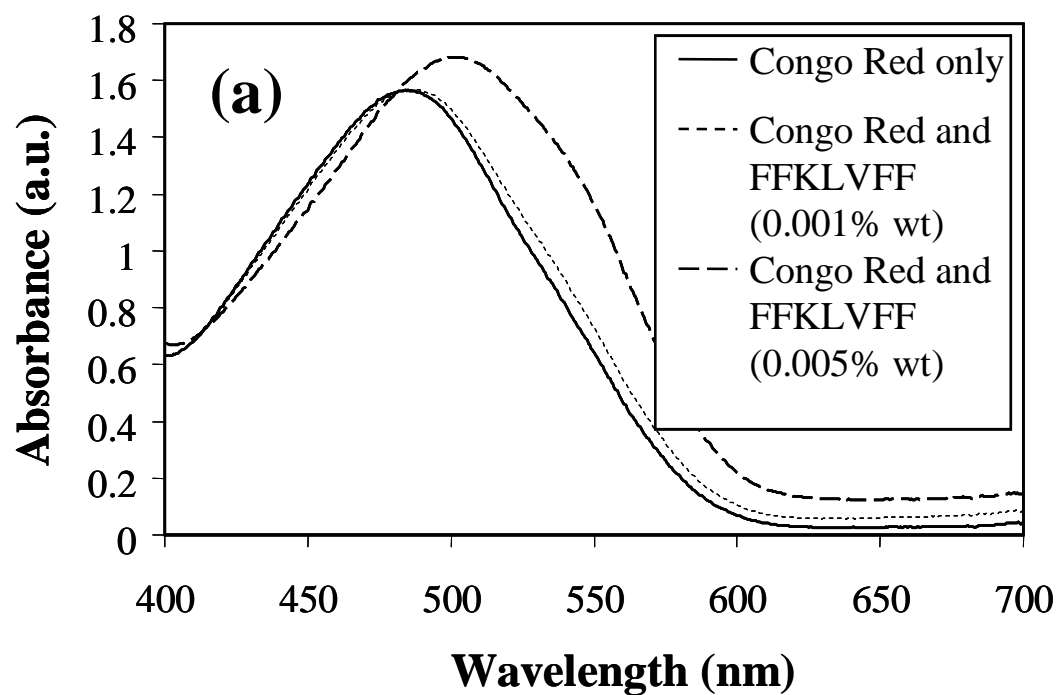**Figure 2**. The UV-Vis spectra of FFKLVFF stained with Congo Red, before (a) and after background subtraction (b) for two different concentrations.
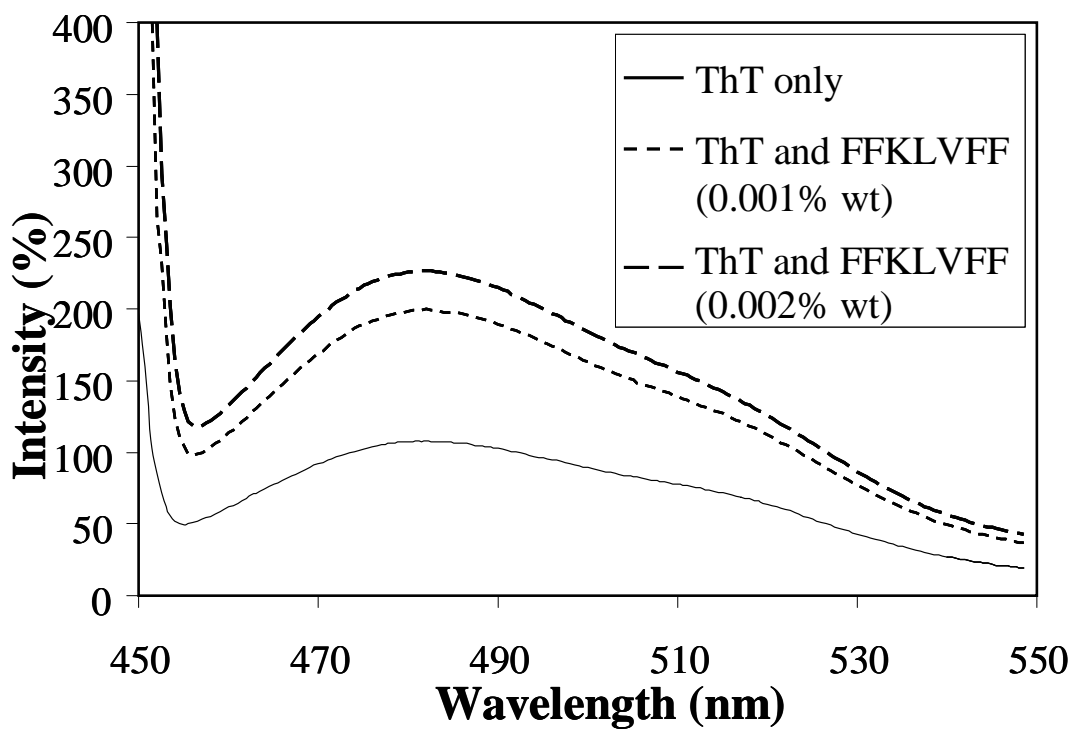
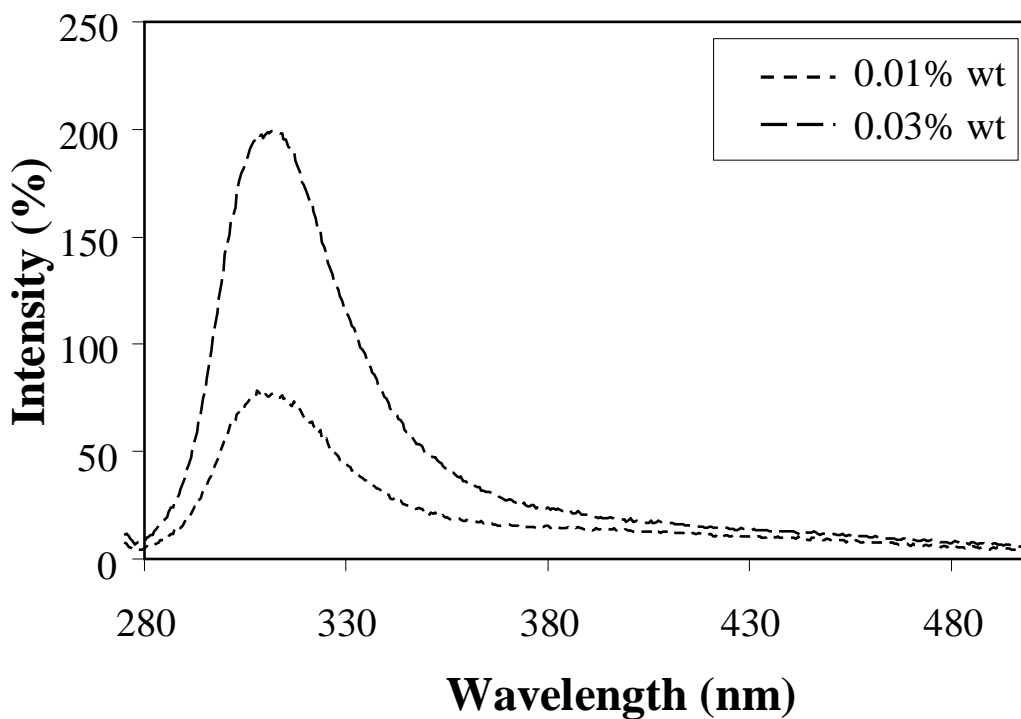**Figure 3** Fluorescence spectra of ThT with and without FFKLVFF
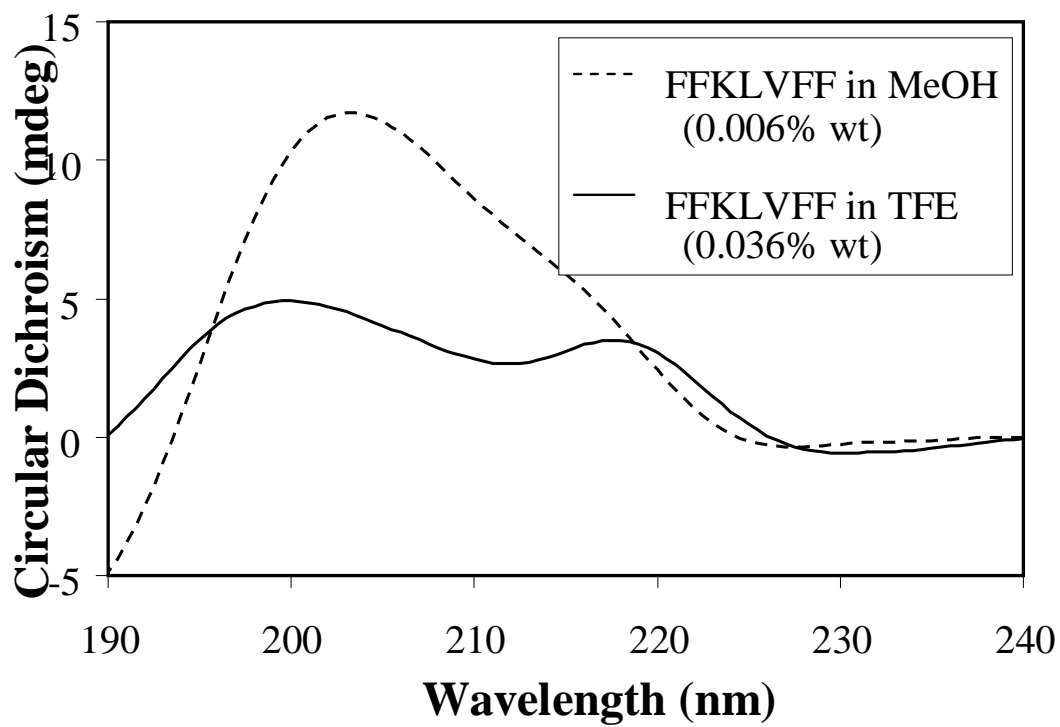

Figure 4 Fluorescence spectra showing aromatic interaction in FFKLVFF

Figure 5. Circular Dichroism (CD) spectra of FFKLVFF in methanol (0.006% wt) and TFE (0.036% wt)
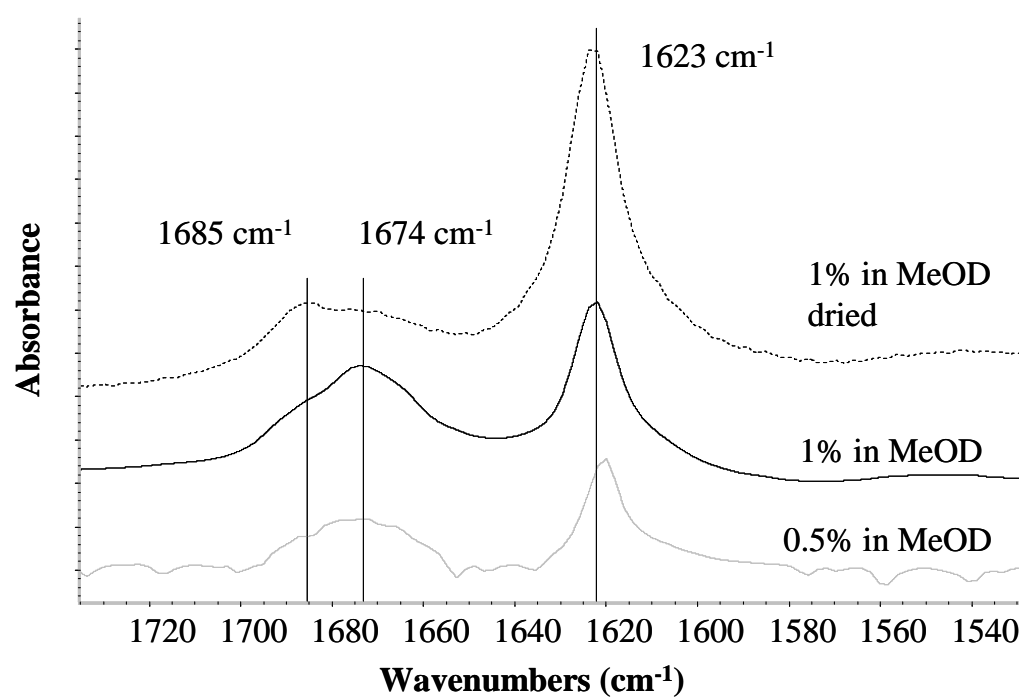
Figure 6. FTIR spectra of the amide I region of FFKLVFF in d_4-methanol (.5% and 1% wt). The solvent spectrum has been subtracted from the spectra of the peptide solutions. The spectrum of the peptide film was also obtained
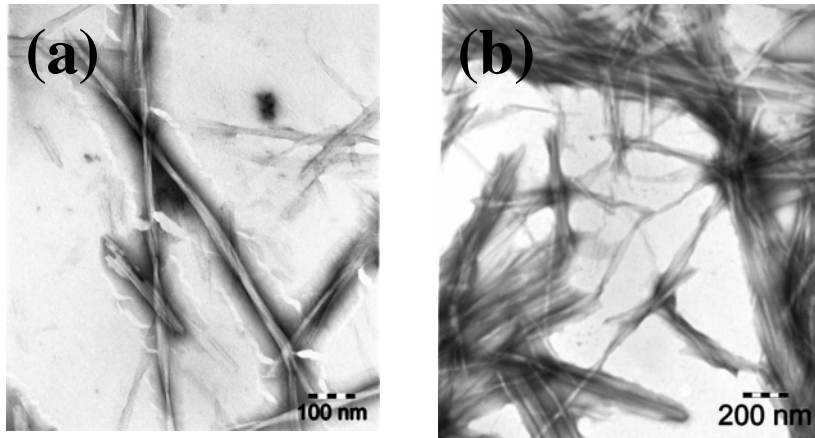
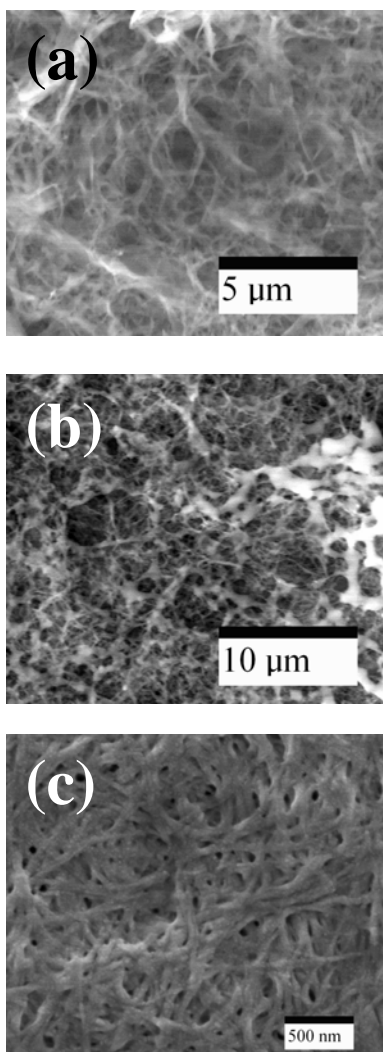**Figure 7**. Representative TEM images of fibrils formed by FFKLVFF in methanol.

Figure 8. Scanning Electron Microscope (SEM) images of dried films of FFKLVFF obtained (a,b) in low vacuum mode and (c) coated with gold in high vacuum mode.

Figure 9. SAXS data and model fit described in text.

TOC Entry